A R C H I V E O F M E C H A N I C A L E N G I N E E R I N G

VOL. LXV 2018 Number 4

DOI: 10.24425/ame.2018.125443

Key words: steam turbine, lifetime assessment, creep, low-cycle

MARIUSZ BANASZKIEWICZ[1], *WOJCIECH RADULSKI*[1], *KRZYSZTOF DOMINICZAK*[1]

ADVANCED LIFETIME ASSESSMENT OF STEAM TURBINE COMPONENTS BASED ON LONG-TERM OPERATING DATA

The paper presents a new method of lifetime calculations of steam turbine components operating at high temperatures. Component life is assessed on the basis of creep-fatigue damage calculated using long-term operating data covering the whole operating period instead of representative events only. The data are analysed automatically by a dedicated computer program developed to handle big amount of process data. Lifetime calculations are based on temperature and stress analyses performed by means of finite element method and using automatically generated input files with thermal and mechanical boundary conditions. The advanced lifetime assessment method is illustrated by an example of lifetime calculations of a steam turbine rotor.

1. Introduction

Over the last years, considerable changes on the power generation market have taken place. They were caused by deregulation of the market and increased share of renewables [1]. It is forecasted that the share of electric power generated by wind and photovoltaic plants will be continuously increasing, which will affect the operation of conventional thermal plants.

Together with the market deregulation and increasing share of wind and sun in energy balance, increased requirements have occurred regarding the flexibility of power generation units, both new designed and the older ones operated for many years [2]. The new requirements include capabilities to switch from based load to cyclic operation, the range and rate of load change and start-up times.

The change of operation mode affects the lifetime of power plant equipment, including steam turbine components. In turbines designed for base load operation, the low-cycle fatigue (LCF), which is important in cyclic operation, has not been

[1] *GE Power Sp.z o.o., 82-300 Elbląg, Stoczniowa 2, Poland.*
Emails: mariusz.banaszkiewicz@ge.com, wojciech.radulski@ge.com, krzysztof.dominiczak@ge.com

considered or taken into account in a simplified way. Additionally, the reduction of start-up times and the increase in loading rates results in augmented fatigue damage of components limiting their service life was not taken into account, either.

An additional aspect which is considered is the trend to extend intervals between overhauls and service life of power generation units. It is dictated by economic factors, but cannot be realized without any technical analyses and at the expense of increased risk of failure. That is why the simultaneous fulfilment of the requirements of flexible operation and lifetime extension creates a need for a broader approach to the problem of lifetime management and optimization. An important element of such an approach is the comprehensive lifetime assessment of steam turbines performed to determine their current technical status and to predict the remaining lifetime.

The advanced lifetime assessment method presented in this paper facilitates a more accurate determination of the residual lifetime as compared with traditional methods. Instead of using finite difference methods with design or representative operating data for the calculation of thermal boundary conditions, the new procedure uses state-of-the-art finite element (FE) method, enhanced methods for thermodynamic and heat transfer calculations using real operating data for the calculation of low-cycle fatigue and creep damage. Due to the higher accuracy, lower safety margins can be used, resulting in less conservative damage estimations and residual lifetime predictions.

2. Advanced lifetime assessment process

The existing lifetime assessment procedure was improved in terms of the input data and the methods used [3, 4]. While in the past the design data were used for evaluation of creep damage, and representative starts were used for the LCF calculation, the new process uses the actual recorded operating data for both processes.

The methods to calculate the stresses in the most critical component has changed from a finite-difference approach to a combined calculation of temperature and stresses via finite-element method.

The improved LTA process is shown in Fig. 1 [3] and each step of the process is explained in the following paragraphs.

The entire LTA process is automated in such a manner that only little manual effort is required for the generation of thermal boundary conditions, the execution of the FE calculations and the determination of numbers of cycles to crack initiation. LTA results and intermediate results from HTC and FE calculation need to be checked for plausibility by means of graphical illustration. This facilitates efficient monitoring of the automated LTA by an experienced engineer. The entire operation history can be considered with reasonable effort. The automation pertains only to the computation of LCF damage, since, depending on the time period, some hundreds of single transient events must be considered, each of them requiring

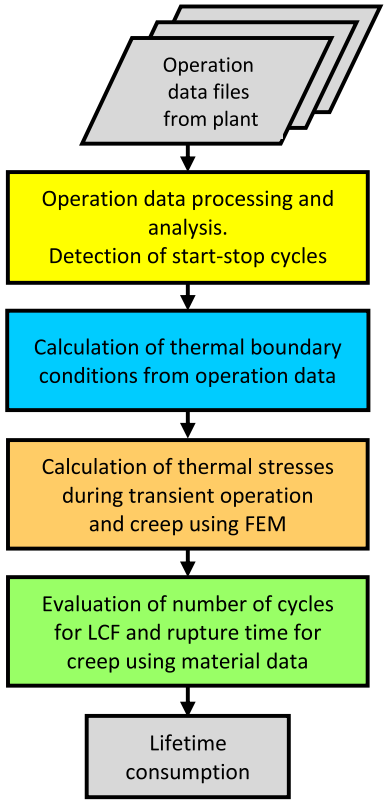

Fig. 1. Advanced lifetime assessment procedure

its own FE calculation. Creep damage on the contrary can be considered with only a few FE calculations. For this reason, the process described in the following considers mainly the determination of LCF damage. After this procedure has been applied to all transient events resulting in the overall LCF damage, LCF and creep damage are accumulated according to the Palmgren-Miner rule.

3. Operating data analysis

One of the major factors influencing the accuracy of lifetime calculations are operating data which are used to prepare thermal and mechanical boundary conditions for finite element analyses (FEA). So far, lifetime assessment studies were based on representative data provided by turbine operators according to special instructions. This approach has been acceptable for base load machines performing slow start-ups, but is not accurate enough in current conditions where many power generation units are operated in cyclic duty or in part/low load regime. Moreover, the variability of start-up conditions in terms of initial metal temperatures and steam temperature and loading rates, makes it very difficult to select one representative

start-up for a given start-up class (i.e., cold, warm, hot and very hot start). In addition to start-up conditions, also shutdown parameters are very important from the point of view of low-cycle fatigue damage, as the stress/strain amplitude is defined using both start-up and shutdown stresses.

For the above reasons, the new methodology of lifetime calculations assumes the use of long-term operating data for describing turbine operation and preparing boundary conditions for FE analyses. The analysis of continuous operating data covering many years of operation (in extreme cases the whole operation time of a unit) is carried out automatically using a dedicated program developed for this purpose. This program is based on data analysis algorithms developed taking into account the experience gained in lifetime assessment studies of a variety of steam turbines.

The analysis of transient operating conditions aims at identifying start-ups and shutdowns, defining their initial thermal conditions, calculating steam-metal temperature differences and temperature rates, and finally preparing input files with the relevant process data required to calculate thermal and mechanical boundary conditions. An example of start-up analysis is shown in Fig. 2, which presents distribution of turbine start-ups with respect to casing initial temperature. The analysis was carried out for a steam turbine of 370 MW power output operating at 535°C live steam temperature and 18 MPa live steam pressure. The inner casing temperature measurement is located in the inlet section and, according to the operating instructions, is representative for the turbine thermal state. Each start and the subsequent shutdown is then described by event plots shown in Fig. 3 enabling visual assessment of the process parameters. The same scope of parame-

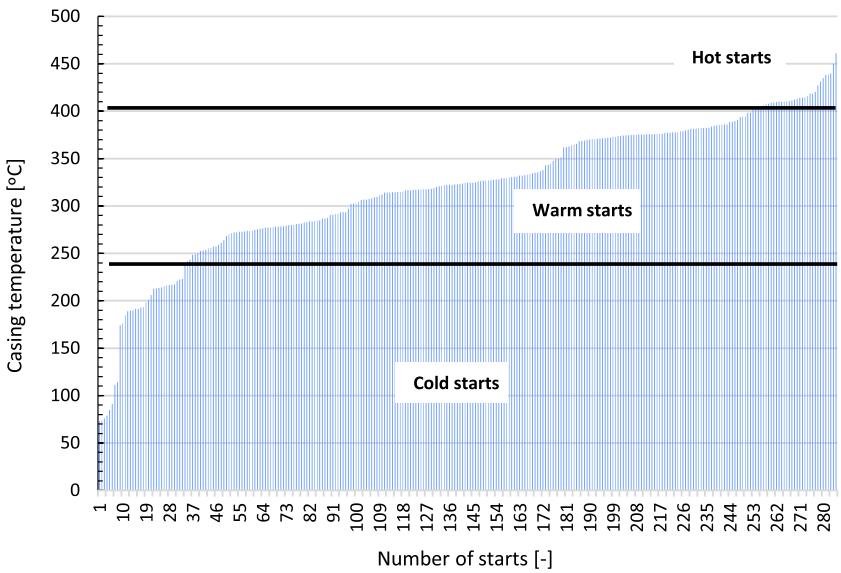

Fig. 2. Distribution of turbine start-ups with respect to initial thermal condition

ters is plotted for start-up (Fig. 3a) and shutdown (Fig. 3b) and includes rotational speed, power output, live and reheat steam temperature and pressure, high- and intermediate-pressure casing and valve chest temperature. A process data file is

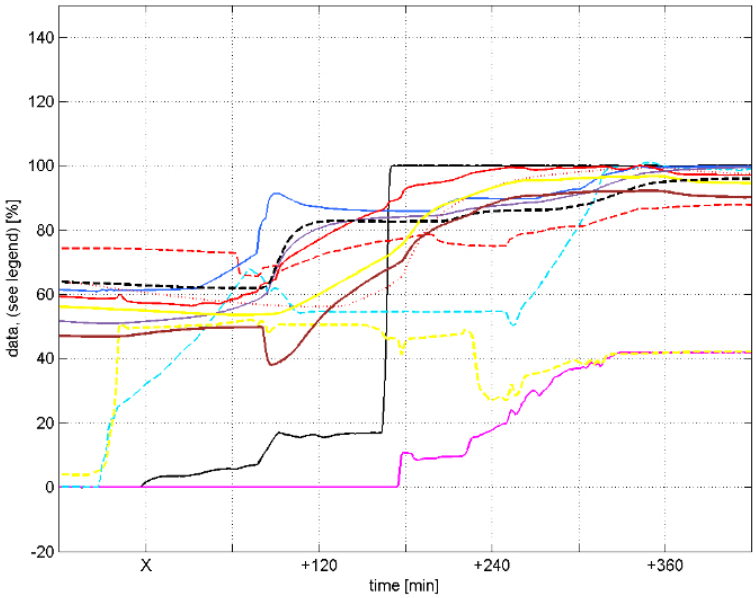

(a)

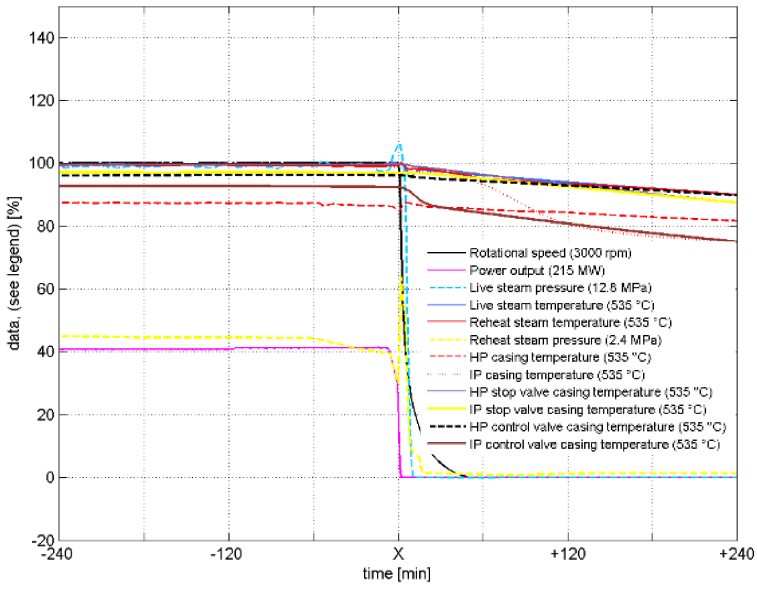

(b)

Fig. 3. Variation of turbine operating parameters during start-up (a) and shutdown (b)

automatically generated for each event plot in the format required by the tool for generating thermal boundary conditions.

The analysis of steady-state service is performed in order to determine the turbine operating conditions at full and part-load which are required for creep damage calculation. In creep analysis, the most important parameter influencing creep damage are operation times at various temperature and load levels. These times are calculated automatically for prescribed temperature, pressure and load ranges and displayed as bar graphs, as shown for example in Fig. 4.

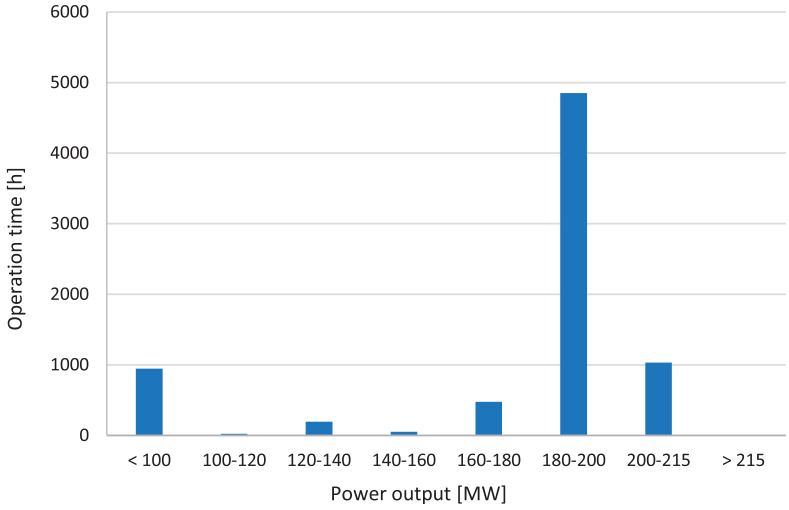

(a)

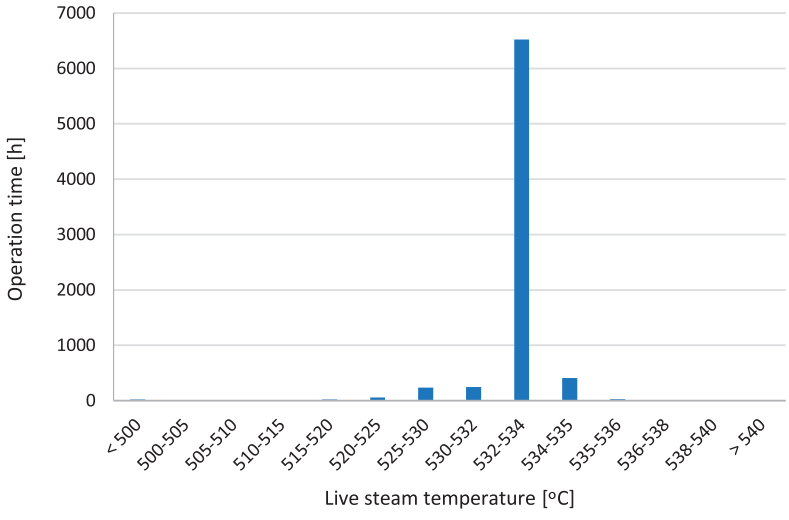

(b)

Fig. 4. Distribution of turbine operation time with different load (a) and temperature (b) ranges

4. Mathematical models

4.1. Heat transfer modelling

Heat transfer in steam turbine components takes place predominantly by heat convection from steam to component surface and by conduction within the component [5]. The convection heat transfer takes place with nonuniform thermal boundary conditions given by steam temperature and heat transfer coefficient. Steam temperature is obtained from thermodynamic calculations of expansion line, and the heat transfer coefficient is a function of geometry and steam parameters in a given region. In steady-state operation, the boundary conditions depend only on the spatial location, while during transient operating conditions both steam temperature and heat transfer coefficient are a function of time [6]. An example of spatial distribution of different types of heat transfer surfaces, where different boundary conditions are applied, is shown in Fig. 5.

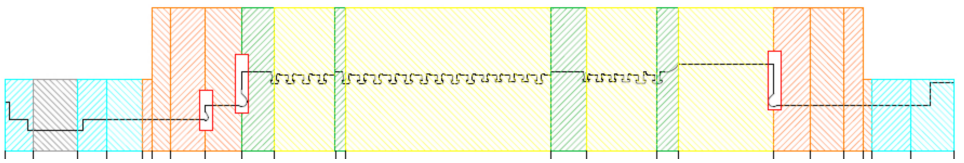

Fig. 5. Heat transfer regions in a steam turbine rotor

Each shaded rectangle represents different heat transfer surfaces where different steam temperature conditions and heat transfer coefficients are applied. In addition, during transient operating conditions, the thermal boundary conditions at each surface vary with time, according to the variation of flow parameters related with turbine run-up or loading. Typical variation of thermal boundary conditions in rotor labyrinth seals during cold start is shown in Fig. 6. It presents variation of steam temperature (Fig. 6a) and relative heat transfer coefficient (Fig. 6b) in selected stages of an intermediate-pressure rotor, where stage 1 is at the inlet and stage 11 at the outlet of the turbine cylinder. Heat transfer in the labyrinth seals is described by the general formula for the Nusselt number, and for turbulent flow the heat transfer coefficient α is calculated using the formula [5]:

$$\alpha = 0.41 \frac{\lambda}{D_h} \mathrm{Re}^{0.7} \left(\frac{\delta}{h} \right)^{0.56}, \tag{1}$$

where: λ is thermal conductivity, D_h is channel hydraulic diameter, Re – Reynolds number, δ – radial clearance, h – channel height. The Reynolds number is calculated from the steam velocity determined on the basis of leakage mass flow rate.

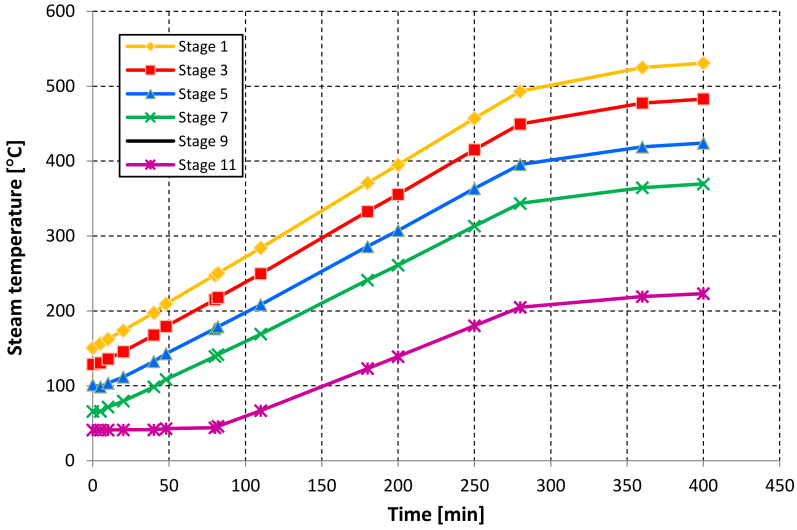

(a)

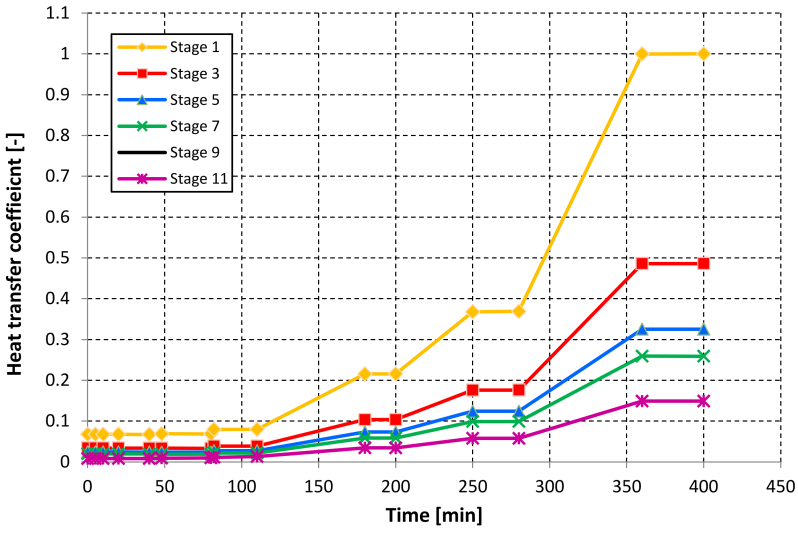

(b)

Fig. 6. Variation of steam temperature (a) and heat transfer coefficient (b) in diaphragm glands of a steam turbine rotor

4.2. Creep model

Creep calculations of turbine rotors, casings and valve chests are performed using a characteristic strain model of creep developed by Bolton [7]. It is a simple model capable of predicting material creep deformation in primary, secondary and

tertiary creep regime. This is a very important and useful feature of the model as design calculations require mean creep behaviour in primary and secondary regime, and residual lifetime analyses are based on minimum creep behaviour in secondary and tertiary regime [8]. The use of the same creep model in design and the remaining lifetime calculations facilitates comparisons of calculation results and model validation.

The equivalent creep strain ε_c is calculated from the following model equation [7]:

$$\varepsilon_c = \frac{\varepsilon_\chi}{\sigma_R/\sigma - 1}, \tag{2}$$

where ε_χ is a characteristic creep strain, which is a material constant at a given time and temperature. The characteristic creep strain can be evaluated using Eq. (2) and by knowing two stresses, i.e., the creep rupture strength σ_{R1} at time t_1 and the stress σ_{D1} to produce datum creep strain ε_{D1} at time t_1. With this assumption, the isochronous stress-strain relation of Eq. (2) can be written as:

$$\varepsilon_c = \frac{\varepsilon_{D1}\,(\sigma_{R1}/\sigma_{D1} - 1)}{\sigma_R/\sigma - 1}. \tag{3}$$

To close the model, a relationship for the rupture strength described by a simple power-law relationship is adopted:

$$\sigma_R = \sigma_{R1}\,(t_1/t)^{1/m}, \tag{4}$$

where m denotes the exponent in the power-law relationship.

The exponent m can be evaluated from two values of rupture strengths at time t_1 and t_2:

$$m = \frac{\log\,(t_2/t_1)}{\log\,(\sigma_{R1}/\sigma_{R2})}. \tag{5}$$

Finally, combining Eqs. (3) and (4), the model relationship between creep strain and time at a constant stress assumes the form:

$$\varepsilon_c = \frac{\varepsilon_{D1}\,(\sigma_{R1}/\sigma_{D1} - 1)}{\dfrac{\sigma_{R1}}{\sigma}\left(\dfrac{t_1}{t}\right)^{1/m} - 1}. \tag{6}$$

The creep model is thus described by three constants:

1) σ_{R1} – creep rupture strength at time t_1,
2) σ_{R2} – creep rupture strength at time t_2,
3) σ_{D1} – stress of creep strain ε_{D1} at time t_1,

which clearly have physical significance and can be derived from readily available data from standard creep tests. This means that no special creep testing is required for using the model for available materials and the sensitivity of creep deformation to rupture and creep strength values exhibiting significant scatter (e.g., for steels typically ±20% of mean value) can be easily studied [9].

The model was evaluated using creep and rupture data of P91 9%CrMo steel produced by the European Collaborative Creep Committee and described by Holdsworth et al. [10]. It was shown that the creep model curves are consistent with the test data and can accurately reproduce the continuously varying slope of the measured curves.

4.3. Elastic-plastic strain determination

In elastic range, when the stress amplitude σ_a is lower than the material yield stress σ_y, the Hooke's law is used and strain amplitude is expressed as [11]:

$$\varepsilon_a = \frac{\sigma_a}{E}, \tag{7}$$

where E is the Young's modulus and σ_a is the stress amplitude calculated using a linear-elastic material model.

As experience shows, thermal stresses at notches calculated using elastic material model can attain very high values exceeding the material yield stress. In traditional approach to fatigue life estimation, in order to determine the number of cycles to crack initiation, it is necessary to know the stresses or strains at notch tip [12]. In such a case, for describing elasto-plastic material response based on the elastic solution, the most commonly used method is the Neuber's rule [13]. The method was derived for a simple state of stress where only one stress component is present at notch tip. For multi-axial state of stress and strain, the Neuber's rule has been extended to [14–16]:

$$\sigma_{eq}\varepsilon_{eq} = \sigma^e_{eq}\varepsilon^e_{eq}, \tag{8}$$

where the superscript e denotes values obtained from elastic solution.

Taking into account the relationship between stress and strain in elastic condition (Eq. (7)) and replacing in Eq. (8) stresses and strains by the appropriate amplitudes, the elastic-plastic strain amplitude is expressed as:

$$\varepsilon_{eq,a} = \frac{\left(\sigma^e_{eq,a}\right)^2}{\sigma_y E}. \tag{9}$$

If strain amplitudes calculated using Eq. (9) are high and result in high damage due to low-cycle fatigue, more accurate FE calculations are performed employing elastic-plastic material model with Prager-Ziegler linear kinematic hardening. The plasticity surface is defined by the function [17]:

$$F = f\left(\sigma_{ij} - \alpha_{ij}\right) - \sigma_y = 0, \tag{10}$$

where $f(\sigma_{ij} - \alpha_{ij})$ is the equivalent stress related to the backstress α_{ij} defining translation of the yield surface. The yield function is traditionally defined as

follows [17]:

$$f\left(\sigma_{ij}-\alpha_{ij}\right)=\sqrt{\frac{3}{2}\left(s_{ij}-\alpha_{ij}^{d}\right)\left(s_{ij}-\alpha_{ij}^{d}\right)}\,, \tag{11}$$

where s_{ij} is a deviatoric part of the stress tensor σ_{ij}, while α_{ij}^{d} is a deviatoric part of the backstress tensor α_{ij}.

The linear kinematic hardening model assumes the associated plastic flow rule in the form [17]:

$$\dot{\varepsilon}_{ij}^{pl}=\dot{W}\frac{\partial F}{\partial\sigma_{ij}}=\dot{W}\left(s_{ij}-\alpha_{ij}^{d}\right), \tag{12}$$

where $\dot{\varepsilon}_{ij}^{pl}$ is a plastic flow rate and $\dot{W}$ denotes here a plastic work. In the linear kinematic hardening model, translation of the yield surface is described by the backstress tensor α_{ij}, whose evolution in time is determined by the Ziegler's linear hardening law [18]:

$$\dot{\alpha}_{ij}=\dot{\mu}\left(\sigma_{ij}-\alpha_{ij}\right), \tag{13}$$

where $\dot{\mu}$ is a positive scalar coefficient given by the formula [19]

$$\dot{\mu}=\frac{C}{\sigma_{y}}\dot{\varepsilon}_{eq}^{pl}\,, \tag{14}$$

where C denotes temperature dependent Ziegler's kinematic hardening modulus, and $\dot{\varepsilon}_{eq}^{pl}$ is an equivalent strain of the plastic flow tensor $\dot{\varepsilon}_{ij}^{pl}$.

4.4. Creep-fatigue damage evaluation

The current degree of damage (lifetime usage) of steam turbine components is determined on the basis of the operating data and mathematical model assumed, describing the process of creep and fatigue damage accumulation. Theoretical damage due to creep and thermal fatigue is determined with the help of the lifetime fractions summation method. In steam turbine practice, a linear model of damage in the form of the linear rule of damage summation is generally used. This rule states that total damage is the sum of creep and fatigue damage and can be written as follows [20]:

$$Z=Z_{B}+Z_{N}\,, \tag{15}$$

where Z_B denotes creep damage and Z_N denotes fatigue damage.

The magnitude of total creep damage Z_B depends on the duration time t of a load at a given temperature and on the magnitude of damage $1/t_B$ in unit time, where t_B is the time to rupture. Its value is derived from the minimum creep curve. According to the linear rule of creep damage accumulation (Robinson's hypothesis), a summation is performed proportionally to the load duration time.

For a set of stresses and temperatures at steady-state operation, the creep damage can be calculated from the following formula [20]:

$$Z_B = \sum_{i=1}^{r} \frac{t_i}{t_{Bi}}, \tag{16}$$

where r stands for the number of stress and temperature levels.

The magnitude of total fatigue damage Z_N depends on the number of load cycles n and the magnitude of damage $1/N$ in each load cycle, where N is the number of cycles to crack initiation. Its value is derived from the minimum LCF curve. According to the linear rule of fatigue damage accumulation (Palmgren's-Miners' hypothesis), a summation is performed proportionally to the number of cycles. For a stress spectrum, which in real turbine operation conditions consists of start-ups from cold, warm and hot states, and from load changes, the fatigue damage is calculated from the following formula [20]:

$$Z_N = \sum_{i=1}^{q} \frac{n_i}{N_i}, \tag{17}$$

where q denotes the number of stress levels.

The linear rule of damage summation has been validated for 1CrMoV rotor steels by Colombo [21], who performed thermal fatigue tests on uniaxial and component feature specimens under service-like conditions. The linear rule resulted in conservative endurance predictions for all specimens but with significantly lower scatter in 3D component-like tests compared with plain and notched thermo-mechanical tests. In the latter tests, the scatter of calculated endurances was considerably lower when the ductility exhaustion rule was used for the creep damage calculation. However, component-like tests simulating high temperature steam turbine rotor operation under real conditions, the time fraction rule used for the creep damage calculation resulted in more accurate endurance predictions compared with the ductility exhaustion rule. Very good accuracy of the linear damage summation rule using the time fraction procedure for the creep damage calculation fully justifies its use in steam turbine component damage assessments.

Theoretically, the computational lifetime is exhausted when the total damage Z reaches one. This critical value, i.e., the value of exhaustion causing failure, is assumed for fatigue cycles, and it denotes crack initiation. Further operation from the instant of crack initiation to the instant of total rupture is associated with an increased risk of failure. In the case of creep damage, the moment that microcracks appear coincides usually with the onset of tertiary creep, which is typically reached after approximately 75% of the time to rupture t_B. Thus, for steam turbine components where creep and fatigue processes occur in parallel, the critical value of 0.75 is assumed [22, 23]. Once this critical value D is reached, an increased risk of cracking occurs and failure possibility increases, and the turbine is further operated with a gradually decreasing safety margin.

5. Lifetime analysis of a steam turbine rotor

The presented method and tools were applied in lifetime calculations of a high-pressure rotor. Continuous operating data for 78 months were delivered by a power plant for analysis. Using the data analysis tool configured for the turbine under investigation, a total of 267 start-ups was detected in the analysed period of time during which the turbine accumulated 43 387 operating hours. Detailed analysis of casing initial temperature resulted in the following numbers of starts:

- 31 cold,
- 214 warm,
- 22 hot starts.

Thermal analysis of the rotor was performed in an axisymmetric model prepared using Abaqus [19] with thermal boundary conditions determined using the methodology described in Section 4.1. Rotor temperature distributions obtained at transient and steady state conditions are presented in Fig. 7. Fig. 7a shows the rotor temperature distribution after 60 minutes of the beginning of a cold start, while Fig. 7b presents its distribution at steady state conditions. A characteristic feature of the transient temperature field are the dominating gradients in radial direction in the rotor inlet sections (red colour) resulting from high steam-metal temperature mismatch and insignificant steam temperature variation in axial direction at the early phase of start-up. When steady state is attained, the axial steam temperature variation and heat transfer coefficients are high, which results in significant rotor temperature gradients in axial direction.

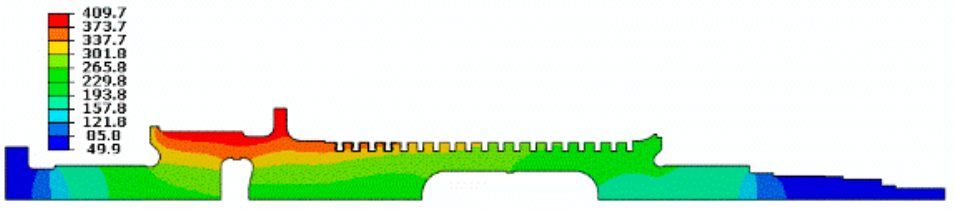

(a)

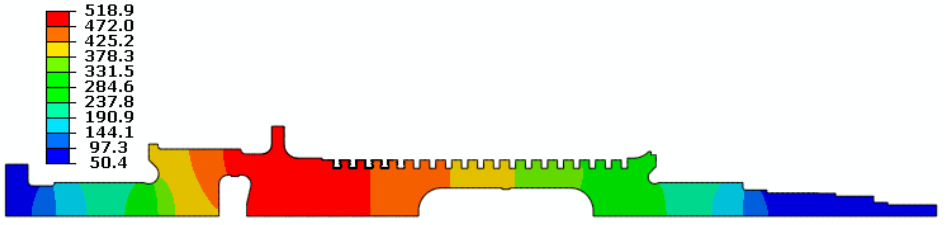

(b)

Fig. 7. Rotor temperature distribution (°C) during a cold start (a) and at steady state (b)

In steady state operation with constant temperature and primary load (rotational speed and steam pressure), stress redistribution and creep strain accumulation take place. The rate of both processes is highest in the areas of stress concentration at high temperature, which results in the largest values of accumulated creep strain. Example distribution of the equivalent creep strain in the rotor after 10000 hours of service at nominal conditions is shown in Fig. 8. The largest area of high creep strain is located below the control stage disc (adjacent to the left cavity) and at its left and right transition radius. These sections of the rotor are thus critical from the point of view of creep damage.

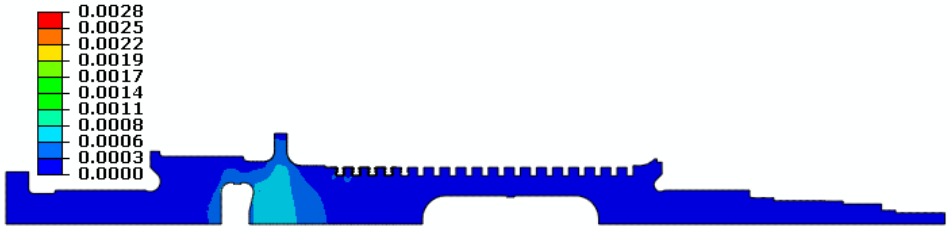

Fig. 8. Creep strain distribution (-) in the rotor after 10000 hours

The analysis of turbine operating conditions performed automatically using the data analysis tool revealed that the turbine was operated in this period with reduced live steam temperature and with two live steam pressure levels: 15÷16 MPa corresponding to part-load operation regime and 17÷18 MPa corresponding to nominal load. This resulted in reduced creep damage comparing with the damage obtained for nominal steam conditions, and consequently lifetime exhaustion was lower than that determined for this operation time at design conditions.

Transient thermal stresses responsible for thermal fatigue damage were calculated using the same axisymmetric model of the rotor as in thermal analysis assuming transient temperature distribution in the rotor as its thermal loading. The locations of highest thermal stresses are also in the sections of highest temperature and thermal gradients. In the analysed rotor, the maximum equivalent stress for all start-up types occurred in the first blades groove. Distribution of relative equivalent stress defined as the ratio of the equivalent stress at a given point to the maximum stress in the rotor is shown in Fig. 9a. A small area of very high stress concentration is seen at the left bottom side of the groove in the transition radius. Consequently, the lowest number of cycles to crack initiation was obtained in this position resulting in the highest low-cycle fatigue damage. It is shown in Fig. 9b presenting distribution of relative number of cycles to crack initiation defined as the ratio of the number of cycles at a given point to the minimum number of cycles in the rotor. The highly localized stress and damage concentration found in the lifetime analyses indicated a possibility of geometry optimization in this area. The existing old groove geometry was modified by applying a stress-optimized shape presently used in new design rotors. The most highly damaged material was removed by

mechanical machining and a new contour was turned at the left bottom side of the groove as shown in Fig. 10b. Comparison of relative stress and fatigue damage for cold start shown in this figure revealed a significant reduction of equivalent stress by nearly 50% and almost sevenfold fatigue life extension as compared with the original groove shape.

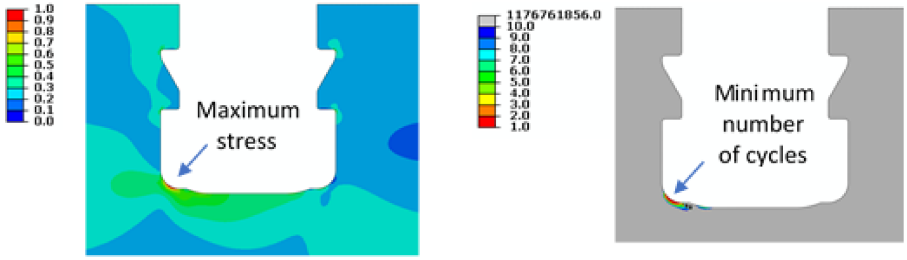

(a) (b)

Fig. 9. Relative equivalent stress distribution (a) and relative number of cycles to crack initiation (b) in the first blade groove

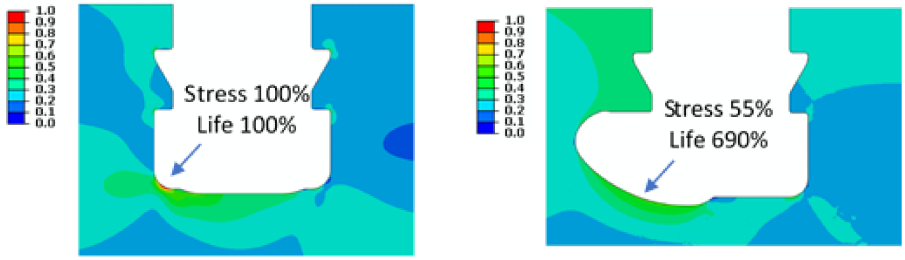

(a) (b)

Fig. 10. Relative stress distribution and fatigue life of the original (a) and optimized (b) blade groove

Accuracy of the advanced lifetime assessment method was investigated by analysing the low-cycle fatigue damage of the blade groove using different methods of damage extrapolation applied so far. For this purpose, all recorded cold start-stop cycles were computed using the finite element method and fatigue damage was obtained for each individual cycle. Fig. 11 presents the low-cycle fatigue damage variation with initial metal temperature. Damage values are given here relative to the fatigue damage obtained for design cold start. The distribution of damage for individual cycles exhibits high scatter reaching 2 orders of magnitude (maximum = 0.22, minimum = 0.0029). Total fatigue damage was then computed with the help of Eq. (17) and this value was assumed as a reference in comparative studies. Fatigue damage was also computed by extrapolating damage due to a single cycle on all considered cold start-ups. It was done by multiplying the unit damage

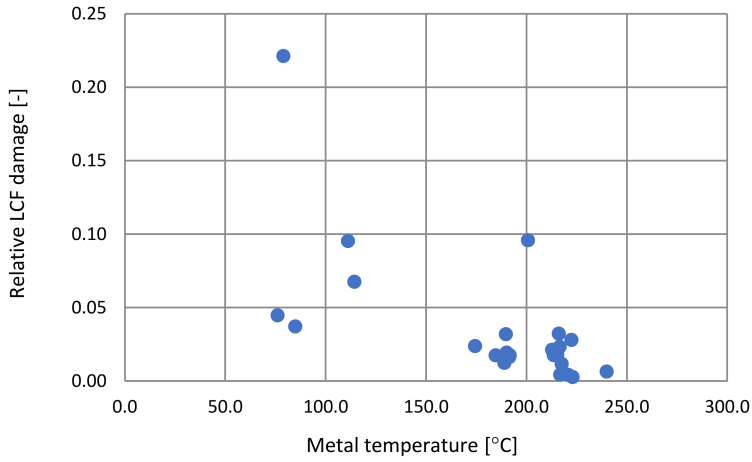

Fig. 11. Relative LCF damage for cold start cycles at various initial temperatures

by the number of cold starts. Three different single cycles were selected for this purpose:

- cold start with minimum initial metal temperature,
- cold start with maximum initial metal temperature,
- cold start with average initial metal temperature.

The results of calculations are shown in Fig. 12 where the LCF damage is scaled with respect to the actual damage computed basing on all cycles (actual relative damage = 1). The two extreme damage values equal 1.27 and 0.19 correspond to a minimum and maximum initial temperature, respectively, and determine the

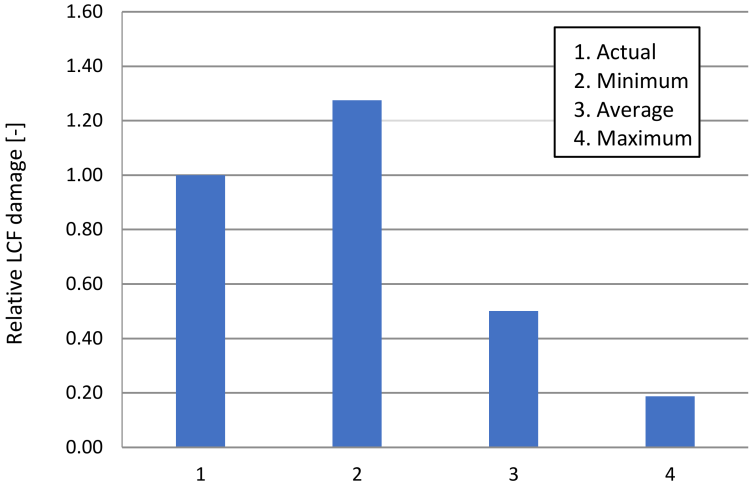

Fig. 12. Relative LCF damage for cold start cycles extrapolated assuming various initial temperatures

scatter in fatigue life of (−27%)÷(+81%). When the cycle with average temperature is used for damage extrapolation, the predicted damage is half the actual value which means that fatigue life is overestimated by 100%. The presented results of damage calculations clearly show a high scatter of fatigue damage for the same class of start-up and high sensitivity to initial thermal conditions. Consequently, lifetime assessment based on only one representative cycle may be fraught with high inaccuracy and lead to wrong predictions of remaining safe operation time of steam turbines.

6. Summary

The described method of advanced lifetime assessment of steam turbines was developed by GE in response to changing market requirements resulting from the increased share of renewables in energy production. The new requirements are related with increased flexibility of steam turbine units operation and extension of their lifetime beyond design limits.

The key factor enabling meeting these requirements is accurate lifetime assessment of turbine critical components. Detailed knowledge about the current status of damage is crucial for both predicting the residual life for unchanged operating conditions and investigating the effect of new service conditions on the turbine lifetime.

The new tools and methods were developed for advanced lifetime assessment of steam turbine components operating at high and significantly changing temperature, like high-pressure rotors, casings and valve chests. By applying the advanced lifetime assessment method and tools it is possible to reliably determine creep-fatigue damage and predict residual life with higher accuracy than it was possible so far.

Creep analysis is performed using the characteristic strain model with material constants specific for a material grade. Low-cycle fatigue analysis is carried out employing elastic and elastic-plastic material models with material data specified for a given material grade. Creep-fatigue damage is evaluated with the help of linear damage accumulation rule which is applied for long-term operating data including many cycles and stress-temperature levels.

Using the example of high-pressure rotor it was shown that fatigue damage can be predicted with errors exceeding 100% when simple analysis of one representative cycle is performed. The highest fatigue damage of the rotor is localized at the first blade groove, which can be improved by applying optimized shape extending the fatigue life by almost 7 times. The above numbers provide evidence of enhanced accuracy of the advanced lifetime assessment methodology and its capabilities of extending remaining life of steam turbines.

Manuscript received by Editorial Board, August 07, 2018;
final version, October 02, 2018.

References

[1] M. Pawlik. Technologically advanced power plant units – new challenges. *Energetyka*, 8:595–599, 2012 (in Polish).

[2] K. Helbig. Steam Plant Case Study: Plant Flexibility Improvements focus ST – minimize variable plant costs. In: *Power Plant Flexibility Europe*, Vienna, 2013.

[3] J. Vogt, T. Schaaf, and K. Helbig. Optimizing lifetime consumption and increasing flexibility using enhanced lifetime assessment methods with automated stress calculation from long-term operation data. In: *ASME Turbo-Expo: Turbine Technical Conference and Exposition*, San Antonio, USA, 3–7 June, 2013. doi: 10.1115/GT2013-95068.

[4] K. Helbig, M. Banaszkiewicz, and W. Mohr. Advanced lifetime assessment and stress control of steam turbines. In: *PowerGen Europe*, Milan, 2016.

[5] T. Chmielniak and G. Kosman. *Thermal Loads of Steam Turbines*, Wydawnictwa Naukowo-Techniczne WNT, Warszawa, 1990 (in Polish).

[6] M. Banaszkiewicz. Numerical investigations of crack initiation in impulse steam turbine rotors subject to thermo-mechanical fatigue. *Applied Thermal Engineering*, 138:761–773, 2018. doi: 10.1016/j.applthermaleng.2018.04.099.

[7] J. Bolton. A "characteristic strain" model for creep. *Materials at High Temperatures*, 25(3):197–204, 2008. doi: 10.3184/096034008X357573.

[8] S.R. Holdsworth. Constitutive equations for creep curves and predicting service life. In: F. Abe, T.U. Kern, R. Viswanathan, editors, *Creep-Resistant Steels*, chapter 14, pages 403–420, Woodhead Publishing Limited, 2008.

[9] M. Banaszkiewicz. Analysis of rotating components based on a characteristic strain model of creep. *Journal of Engineering Materials and Technology*, 138(3):031004-1-11, 2016. doi: 10.1115/1.4032661.

[10] S.R. Holdsworth, M. Askins, A. Baker, E. Gariboldi, S. Holmström, A. Klenk, M. Ringel, G. Merckling, R. Sandstrom, M. Schwienheer, and S. Spigarelli. Factors influencing creep model equation selection. *International Journal of Pressure Vessels and Piping*, 85(1-2):80–88, 2008. doi: 10.1016/j.ijpvp.2007.06.009.

[11] M. Banaszkiewicz. Online monitoring and control of thermal stresses in steam turbine rotors. *Applied Thermal Engineering*, 94:763–776, 2016. doi: 10.1016/j.applthermaleng.2015.10.131.

[12] W. Guo, C.H. Wang, and L.R.F. Rose. Elastoplastic analysis of Notch-Tip Fields in Strain Hardening Materials. Aeronautical and Maritime Research Laboratory Report, DSTO-RR-0137, Melbourne, Australia, 1998.

[13] H. Neuber. Theory of stress concentration for shear-strained prismatic bodies with arbitrary nonlinear stress-strain law. *Journal of Applied Mechanics*, 28(4):544–550, 1961. doi: 10.1115/1.3641780.

[14] M. Hoffman and T. Seeger. A generalized method for estimating multi-axial elastic-plastic notch stresses and strains, Part 1: Theory. *Journal of Engineering Materials and Technology*, 107(4):250–254, 1985. doi: 10.1115/1.3225814.

[15] M. Hoffman and T. Seeger. A generalized method for estimating multi-axial elastic-plastic notch stresses and strains, Part 2: Application and general discussion. *Journal of Engineering Materials and Technology*, 107(4):255–260, 1985. doi: 10.1115/1.3225815.

[16] A. Moftahar, A. Buczyński, and G. Glinka. Calculation of elasto-plastic strains and stresses in notches under multiaxial loading. *International Journal of Fracture*, 70(4):357–373, 1995. doi: 10.1007/BF00032453.

[17] T. Bednarski, *Mechanics of plastic flow*, PWN, Warsaw, 1995 (in Polish).

[18] H. Ziegler. A modification of Prager's hardening rule. *Quarterly of Applied Mathematics*, 17:55–65, 1959.

[19] *ABAQUS 6.12 User Manual*

[20] M. Banaszkiewicz. Multilevel approach to lifetime assessment of steam turbines. *International Journal of Fatigue*, 73:39–47, 2015. doi: 10.1016/j.ijfatigue.2014.10.009.

[21] F. Colombo. *Service-like thermo-mechanical fatigue characteristic of 1CrMoV rotor steel*. Ph.D. Thesis, Swiss Federal Institute of Technology, Zurich, Switzerland 2007. doi: 10.3929/ethz-a-005415280.

[22] Lifetime Assessment Instruction, ALSTOM Power, Baden, 2007.

[23] K. Mazur-Buyko. Computational methods of lifetime determination of steam turbine casings and rotors. In: *1st Scientific-Technical Session "Lifetime of steam turbine components and methods of its prediction"*, pages 42–53, 1986 (in Polish).